Effect of annealing temperature in improvement The optical properties of TiO_2 doped Fe_2O_3 to use in thin film

.

ABSTRACT

Solar energy is already has being widely successfully used in residential and industrial setting for thermal and electrical application such as space technology, communication, etc. I **Aims:** The aim of this study the effect of the annealing temperature in improvement optical properties of titanium oxide nanostructure doped iron oxide for use in thin film.

Study design: The spray pyrolysis deposition method used for preparation the nanostructure material.

Place and Duration of Study: This study was conducted in department of physics and department of materials sciences, Al-neelain university, between January 2016 and January 2019.

Methodology: Thin films of Titanium Oxide ($TiO_{2)}$ doped Iron Oxide (Fe_2O_3) have been prepared by chemical spray pyrolysis deposition technique. A laboratory designed glass atomizer was used for spraying the aqueous solution. Which has an output nozzle about 1 mm. then film were deposited on preheated cleaned glass substrates at temperature of 400 ^{O}C. we used different concentration to study optical parameters. A 1.5g TiO2 powder of anatase structure doped with 1.5 g of Fe_2O_3 was mixed with 2 ml of ethanol and stirred using a magnetic stirrer for 30 minutes to form TiO_2 paste to obtain the starting solution for deposition and spray time was 10 s and spray interval 2 min was kept constant. The carrier gas (filtered compressed air) was maintained at a pressure of 10^5 Nm^{-2}, and distance between nozzle and substrate was about 30 cm ± 1 cm. Thickness of sample was measured using the weighting method and was found to be around 400nm. Optical transmittance and absorbance were record in wavelength range of (200-1100) nm using UV-Visible spectrophotometer (Shimadzu Company Japan).

Results: The results obtained showed that the optical band gap decreased from 5.6eV before annealing to (3.9 , 3.26 , 3.24 and 3.27 eV) after annealing temperature at(450^o – 500^o) for TiO_2:Fe_2O_3 thin films, this result refer to the broadening of secondary levels that product by TiO_2: doping to the Fe_2O_2thin films. Also the results showed the variation of refractive index with wavelength for different concentration after annealing temperature at (450^o – 500^o) of $TiO_{2:}$ Fe_2O_3 films from this figure, it is clear that n decrease with low concentration and increase with high concentration after annealing temperature that mean the density is decreased of this films. In addition the extinction coefficient of TiO_2:Fe_2O_3 thin films recorded before annealing and with different concentration (1.1, 1.2, 1,5 and 1,6) and in the range of (300 – 1200) nm and at annealing temperature from (450^o – 500^o). It observed from that the extinction coefficient, decrease sharply with the increase of wavelength for all prepared films and all the sample after annealing is interference between them accept the sample before annealing is far from the other sample.

Conclusion: The TiO_2 thin film shows better result after annealing; By exposing temperature during annealing process degree at (450^o- 500^o) is found to be the best temperature for annealing TiO_2 thin film. The study concluded that an annealing temperature Contributes to the improvement of optical properties related to increasing the efficiency of the solar cell, especially the refractive index, energy gap, extinction coefficient.

Keywords: annealing, pyrolysis, nanostructure, extinction coefficient, band gap

1. INTRODUCTION

Solar energy can be harvested either by deriving directly from sunlight or by indirect methods [1][2]. Gra¨ tzel and his co-workers developed a solar cell by combining nanostructured electrodes and efficient charge injection dyes with energy conversion efficiency exceeding 7% in 1991 to 10% in 1993 this solar cell is called dye-sensitized nanostructured solar cell or the Gra¨ tzel cell. A dye-sensitized solar cell (DSSC) is another version of energy conversion device other than common solar cell which is silicon solar cell. DSSC can be made with lower cost because of its simple manufacturing techniques [3]. The basic structure of DSSC consists of two conducting glass electrodes as a sandwich arrangement. These electrodes are transparent, which allows the light to pass through it DSSC consist of three main components: photo anode, redox couple electrolyte, and counter electrode. In principle, the operation of DSSCs is based on the injection of electrons from a dye to a metal oxide photoanode by using a photoinduced process [3]. The important means of producing high-efficiency solar cells are reducing reflectance, trapping light in the cell and increasing light absorption. Silicon solar cells have achieved electricity conversion efficiencies ranging from 15% to 20%. However, the high fabrication cost and the usage of toxic chemicals in producing highly purified silicon during the manufacturing process has motivated the search for an environmentally friendly, low-cost solar cell [4]. Dye-sensitized solar cells (DSSC) have received considerable attention since O'Regan and Grätzel reported a remarkably high conversion efficiency of nearly 10% using nanocrystalline mesoporous TiO_2 film. However, these organic solar cells are still limited to low power conversion efficiencies [4].Dye-sensitized solar cell (DSSC) less efficient in power conversion than solar cells made from Si or other semiconducting materials and have been considered as an alternative to silicon-based solar cells, which have been commercialized for more than 50 years, due to their low cost and unique characteristics such as transparency, simple fabrication procedure, and promising efficiency Thus, researchers have an increased interest in developing this kind of photovoltaic cell in recent years[5,6, 7].

Dye-sensitized solar cells operate differently from other types of solar cells in many ways with some remarkable analogies to the natural process of photosynthesis. Therefore, this system has repeatedly been described in terms of artificial photosynthesis since the interest in DSSC took off with the landmark publication by O'Regan and Gr¨atzel in the early 1990 like the chlorophyll in plants, a monolayer of dye molecules (sensitizers) absorbs the incident light, giving rise to the generation of positive and negative charge carriers [7]. This process involves the regeneration of Oxidized dyes by accepting an electron donor from the electrolyte and the reduction of an electron acceptor in the electrolyte at the counter-electrode surface. In DSSC photogenerated charge carriers from dye molecules are collected by photoanode and counter-electrode material which transfer these charge carriers (electrons) to the outer circuit[9,10,11]. DSSC converts visible light into electricity based on the sensitization of wide band gap semiconductors and is primarily comprised of photoelectrode, redox electrolyte and counter electrode. Other materials include transparent conducting oxide and sealing agents. DSSC components have gone under various developments over the years in order to enhance the efficiency of the cell [13]. A typical DSSC consists of a transparent conductive oxide (TCO), semiconductor oxide, dye sensitizer, electrolyte and counter electrode. The working electrode is a nanoporous semiconductor oxide that is placed on conducting glass and is separated from the counter electrode by only a thin layer of electrolyte solution. The extension of the photoelectrode dye enables the collection of lower-energy photons [14].

TCO substrates must be highly transparent to allow the maximum passage of sunlight to the active area [15]. Typically, DSSC are constructed with two sheets of TCO material as current collectors for the deposition of the semiconductor and catalyst [16]. The TCO material

characteristics determine the efficiency of DSSC [17]. due to the efficient charge transfer of electrical conductivity to minimize energy losses. Fluorine tin oxide (FTO, SnO2:F) and indium tin oxide (ITO, In2O3:Sn) are typical conductive oxide substrates consisting of soda lime glass coated with fluorine tin oxide or indium tin oxide, respectively. The transmittance of ITO films are over 80% in the visible region, with a sheet resistance of approximately 18 Ω/cm2, whereas FTO films exhibit a transmittance of approximately 75% with a sheet resistance of 8.5 Ω/cm2. Sima et al. conducted a study based on FTO and ITO glass substrates sintered at 450 ºC [17]. They found that upon sintering, the sheet resistance of ITO increased from 18 Ω/cm2 to52 Ω/cm2, while the sheet resistance of FTO remained constant. The overall conversion efficiencies of DSSC based on FTO and ITO are approximately 9.4% and 2.4%, respectively. Thus, FTO is strongly recommended for use in DSSC fabrication due to its conduction properties and stable sheet resistance temperature [17].

2. MATERIAL AND METHODS

2.1 Preparation of the TiO_2 films

TiO_2 thin film prepared by spray pyrolysis deposition (SPD) method which involves spraying the solution onto substrate placed over a heated surface where the solvent will evaporate to form a solid chemical compound. The compound used to produce a thin film by this method should be volatile at the temperature of deposition. Thin films of Titanium Oxide (TiO_2) doped Iron Oxide (Fe_2O_3) have been prepared by chemical spray pyrolysis deposition technique Iron oxide thin films of hematite, maghemite, magnetite and wustite have been prepared by a variety of techniques including chemical vapor deposition (CVD), sputtering, sol-gel, pulsed laser deposition (PLD), molecular beam epitaxy (MBE) and spray pyrolysis. The quality of the film depends on the technique of growth and diverse operating parameters. Iron oxide (α-Fe_2O_3) or commonly known as hematite is a semiconductor material which has been extensively studied for many applications because it is a cheap nontoxic, thermodynamically stable and abundant material with promising optical properties. Iron oxide (α-Fe_2O_3) is used as a dye at different concentration. 1.5 mg of Fe2O3 is dissolved in 2mL of Ethanol. The dye solution is stirred at room temperature for 30 minutes in magnetic stirrer. The TiO2 coated FTO substrates were soaked in the dye solution for 15 min. The dye sensitized electrode in different concentration was prepared for all the samples by this method. A laboratory designed glass atomizer was used for spraying the aqueous solution. Which has an output nozzle about 1 mm. then film were deposited on preheated cleaned glass substrates at temperature of 400^{O}C. we used different concentration to study optical parameters. A 1.5 mg TiO_2 powder structure doped with 1.5 mg of Fe_2O_3 was mixed with 2 ml of ethanol and stirred using a magnetic stirrer for 30 minutes to form TiO_2 to obtain the starting solution for deposition and spray time was 10 s and spray interval 2 min was kept constant. The carrier gas (filtered compressed air) was maintained at a pressure of 105 Nm^{-2}, and distance between nozzle and substrate was about 30 cm ± 1 cm.The spraying was done by making a left and right motion until all of the solution was deposited onto substrates. After the spraying process was done, the TiO_2 films that had been fabricated were put in the furnace for annealing process. The temperature was set at (450^{o} and 500^{o}). The period for annealing is 30 minute. Then, the samples were taken out from the furnace and let to cool down to room temperature before dipped into the dye.

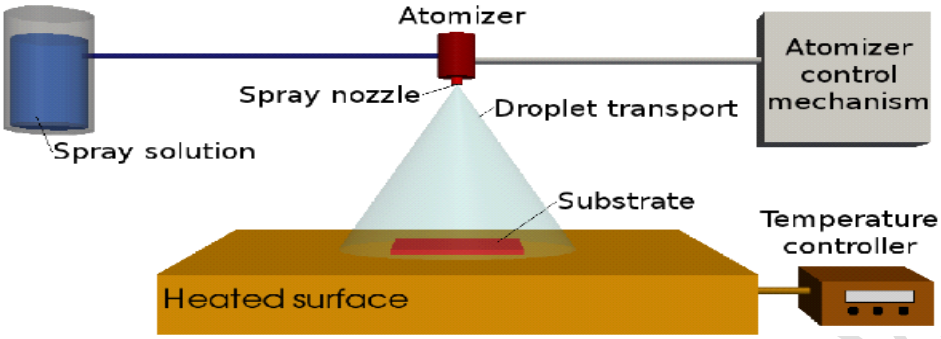

Fig.1. Spray pyrolysis deposition technique

2.2 DSSC Characterization

The XRD patterns were recorded on a Philips X'pert Pro MPD model X-ray diffractometer using Cu Kα radiation as the X-ray source. The diffractograms were recorded in the 2θ range of 10- 80º. The average crystallite size of anatase phase was determined according to the Scherrer equation. The morphology and size of nanopowders and films were characterized using scanning electron microscope (SEM) (JEOL JSM-7600F, Japan - 30JSM) equipped with an energy dispersive X-ray (EDS). The absorption spectra of dye solutions and dyes adsorbed on TiO2 surface were recorded using a UV–vis spectrophotometer (Shimadzu, model UV-4200).

2.2.1 XRD characterization

Various structural parameters of the TiO_2 photoanode developed on ITO coated glass substrates at different annealing temperatures (450 °C, 500 °C) were investigated by X-ray diffractometer (GBC-EMMA, Australia) at 2_ position (from 20° to 90°) with CuK_ X-ray of wavelength - = 1.54056 Å.

2.2.2 SEM characterization

SEM characterizations were carried out by FESEM (JEOL JSM-7600F, Japan) at 5 kV to 7 kV accelerating voltage

2.2.3 UV-ViS-Spectrophotometer

UV-Vis- spectra of TiO_2 films annealed at different temperatures were recorded by UV-Vis-NIR spectroscopy (Hitachi 4200, Japan)

3. RESULTS AND DISCUSSION

3.1 Microstructure and morphological characteristic of the TiO_2 electrodes

The XRD patterns of TiO2 NPs at different calcination temperatures are shown in Figure 2. The nanocrystalline anatase structure was confirmed by (1 0 1), (0 0 4), (2 0 0), (1 0 5) and (2 1 1) diffraction peaks [(31)]. The XRD patterns of anatase has a main peak at 2θ = 25.28 corresponding to the 101 planes (JCPDS 21-1272) while the main peaks of rutile and brookite phases are at 2θ = 27.48 (110 plane) and 2θ = 30.88 (1 2 1 plane). The prominent peaks representing anatase phase of nanocrystalline TiO2 powder used for this study can

be seen at the 2θ values of 25.28, 37. 80, 48.05, 53.89, 55.06, 62.69, 68.76, 70.31 and 75.03 .

The (101) peak of anatase becomes sharper and stronger with enhancing the annealing temperature from 500 to700 °C. It is reasonable to speculate that the mesostructures of TiO2 NPs reconstructed along with the increase of crystallite size and crystallinity. Namely, the internal surface area of the TiO2 film decreased with enhancing the annealing temperature, which is consistent with previous observation [32]. This decrease in the internal surface area of TiO2 film can also be confirmed by the decreasing absorbed amount of N719. The improvement in the crystallinity, decreases in the internal surface area, and the adsorbed amount of N719 will certainly affect the properties of DSSCs, which will be discussed further in the following section. Our observations indicate that the particles have relative high crystallinity, which is beneficial for the improvement of photoelectrochemical properties of its corresponding film electrode. The amount of rutile in the samples was estimated using the Spurr equation [33]:-

$$FR = 1\ \{1 + [0.8 I_A (101)/I_R (110)]\} \quad \ldots\ldots\ldots\ldots\ldots (1)$$

Where FR is the mass fraction of rutile in the samples, IA(1 0 1) and IR(1 1 0) are integrated main peak intensities of anatase and rutile, respectively. Results shows the phase transformation from anatase to rutile starts in 600 0C. In addition to the anatase-to-rutile phase transformation, the average anatase crystallite size, as determined by applying the Scherrer equation to the anatase (101) peak, increased from 13 to 42 nm, about 70%, over the temperature range from 500 to 700 °C.

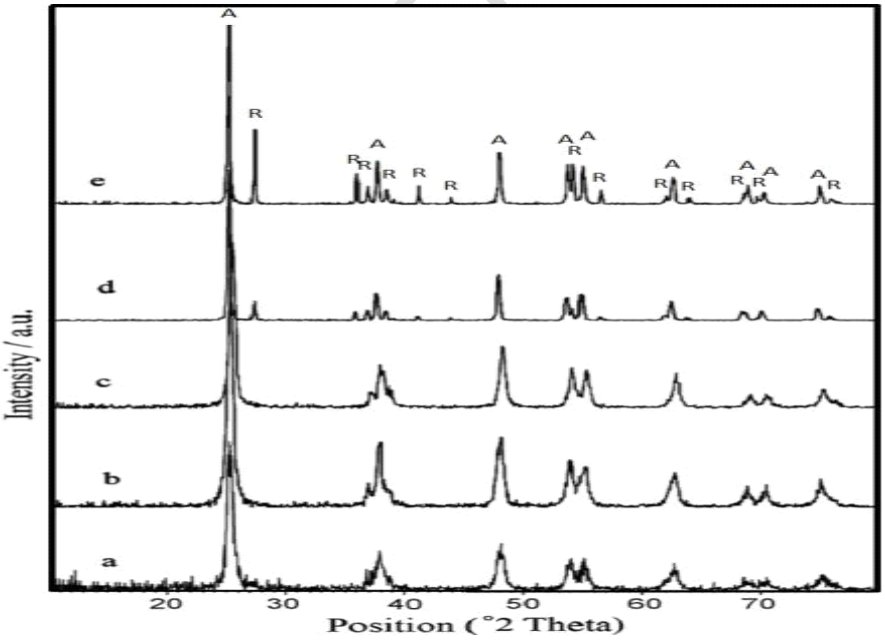

Fig.2. XRD patterns of undoped and after doped TiO_2 nanoparticles calcinated at different concentration at annealing temperature(450^o – 500^o): (a) before, (b) 1.1mol/L, (c) 1.2mol/L, (d) 1.5mol/L, (e) 1.6mol/L (A).

Fig. 3 shows the scanning electron micrograph of a typical TiO_2 (anatase) film deposited by screen printing on a conducting glass sheet that serves as current collector. The film thickness is typically 5–20 m and the TiO_2 mass about 1–4 mg/cm2. Analysis of the layer morphology shows the porosity to be about 50–65%, the average pore size being 15 nm. The prevailing structures of the anatase nanoparticles are square–bipyramidal, pseudocubic and stablike. According to HRTEM measurements the (1 0 1) face is mostly exposed followed by (1 0 0) and (0 0 1) surface orientations. A recent alternative embodiment of the DSC concept is the sensitized heterojunction usually with an inorganic wide band gap nanocrystalline semiconductor of n-type polarity as electron acceptor, the charge neutrality on the dye being restored by a hole delivered by the complementary semiconductor, inorganic or organic and of p-type polarity. The prior photo-electrochemical variant, being Further advanced in development, has an AM 1.5 solar conversion efficiency of over 10%, while that of the solid-state device is, as yet, significantly lower.

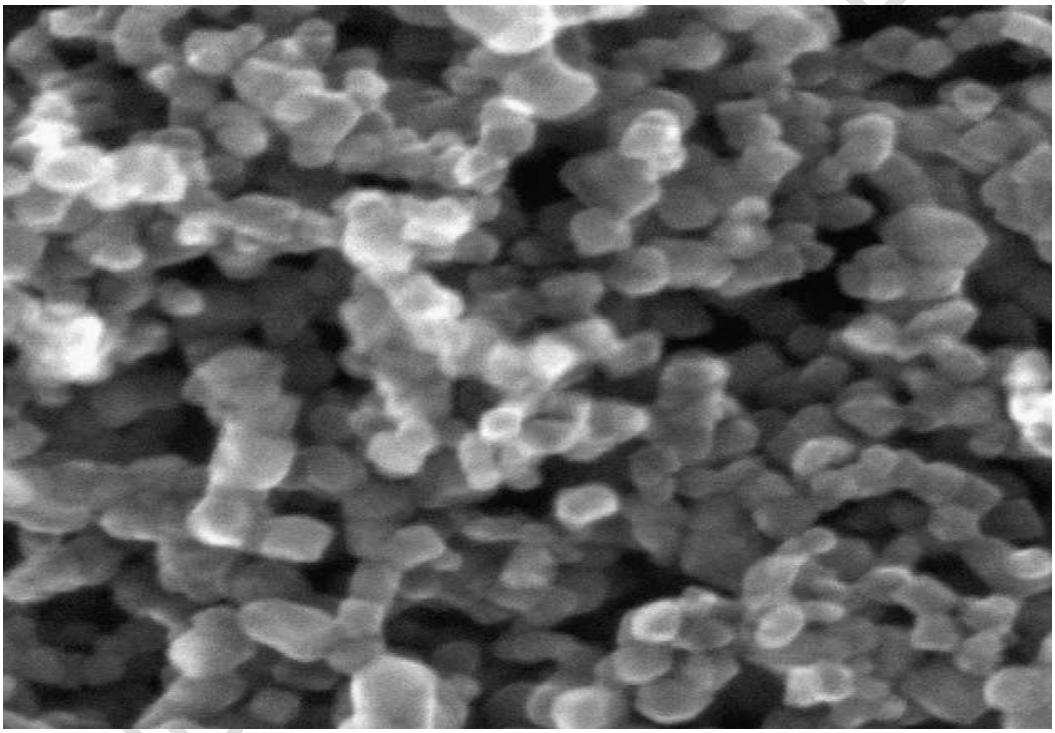

Fig.3. Scanning electron microscope picture of a nanocrystalline TiO_2 (anatase) film used in the dye-sensitized solar cell (DSSC)

Analysis of optical absorbance spectra (A) , transmission (T) and reflectance (R) is one of the most productive tools for understanding the band structure and energy band gap (E_g) of both amorphous and polycrystalline materials. To study effect thermal annealing on optical absorbance of TiO_2: Fe_2O_3 thin films the dependence of absorbance on the wavelength (λ) in the spectral range of (200 -1000) nm, was recorded. Fig (4), Fig (5) and Fig (6) are representing the relationship between the absorbance, transmittance and the reflectance with wavelength respectively. From Fig(3) represent absorbance spectra at concentration at (1.1, 1.2, 1.5 and 1.6) respectively at annealing temperature (450o-500^o) it can notice that high value of absorbance spectra increase at concentration (1.2mol/L) and we found peak is very big broadening but found interference between concentration(1.1, 1.5 and 1.6 mol/L) respectively and peak is very small sharp.

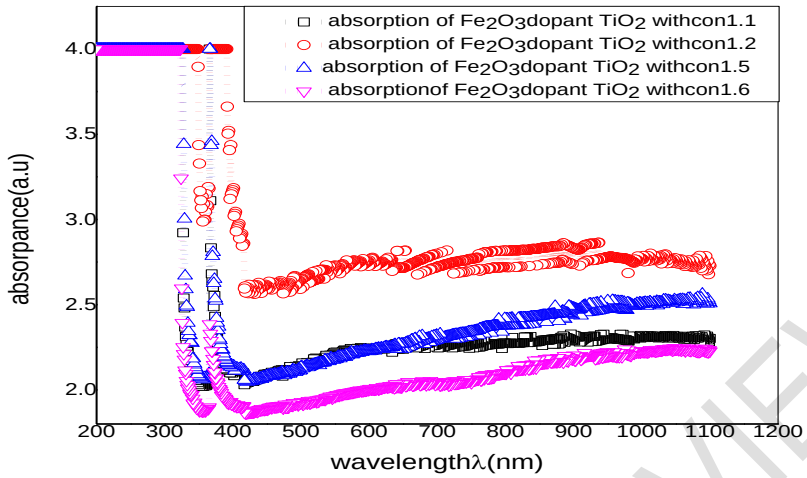

Fig.4. Absorption vs wavelength plot of Fe_2O_3doped TiO_2 thin films at concentration (1.1, 1.2, 1. 5 and 1.6mol/L) at annealing temperature at (450^o-500^o)

From fig (5) it can be notice that the transmittance spectra before annealing is a high value but is an improving after annealing temperature it shows that transmittance spectra increase with decrease concentration and decrease with increase concentration

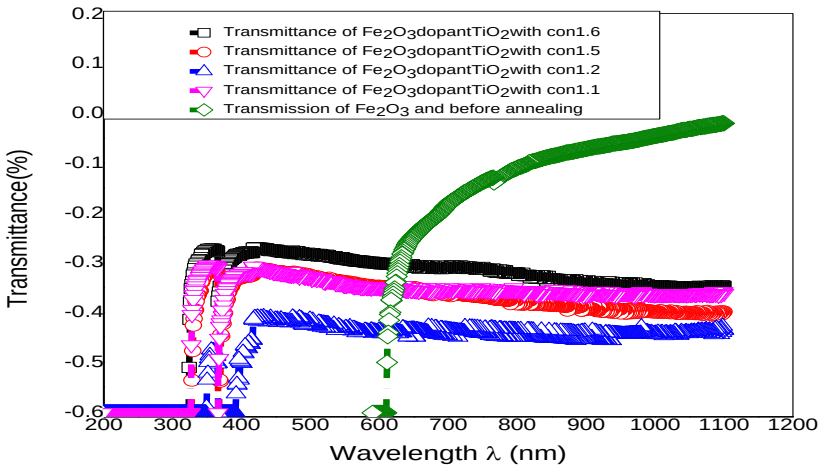

Fig.5. Transmission vs wavelength plot of Fe_2O_3 before and after doped TiO_2 thin films with concentration (1.1, 1.2, 1.5 and 1.6mol/L) at annealing temperature at (450^o-500^o)
From fig (6) it can be notice that reflectance decrease with high concentration and increase with low concentration but the reflectance is increase from the wave length 300nm until to the wave length 350nm and return back another from wavelength from 360-400nm then become stable.

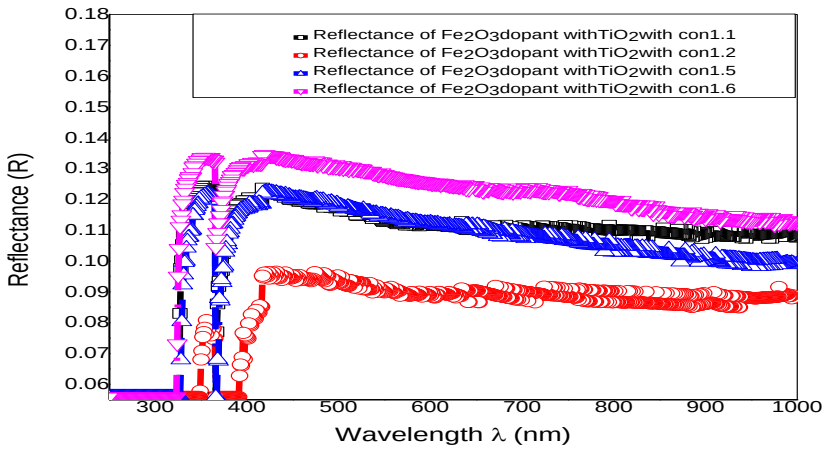

Fig.6.Reflectance vs wavelength plot of Fe_2O_3dopedTiO$_2$ thin films with concentration (1.1, 1.2, 1.5 and1.6mol/L) at annealing temperature (450^o- 500^o)

The absorption coefficient α(λ) of the annealed TiO_2: Fe_2O_3 thin films can be calculated by simple method from transmittance spectra and defined as equation :

$$T = exp\,[-\alpha\,(\lambda)\,d] \qquad \ldots\ldots\ldots\ldots\ldots\ldots\ (2)$$

Where T is the optical transmittance and d is the thickness of TiO_2:Fe_2O_3 thin films A plot of absorption coefficient vs wavelength is shown in fig (7). From this figure it can notice that the absorption coefficient is increase with gradually with photon energy until 4eV. While the increases of α become sharply and we show found interference at incident photon energy equal 4eV. In addition from this figure it can notice clearly the α increases with high concentration after annealing temperature and high value of α refer to the allowed direct transition for all prepared TiO_2:FeO_3 and at concentration 1.2mo/L the absorption coefficient is not shining.

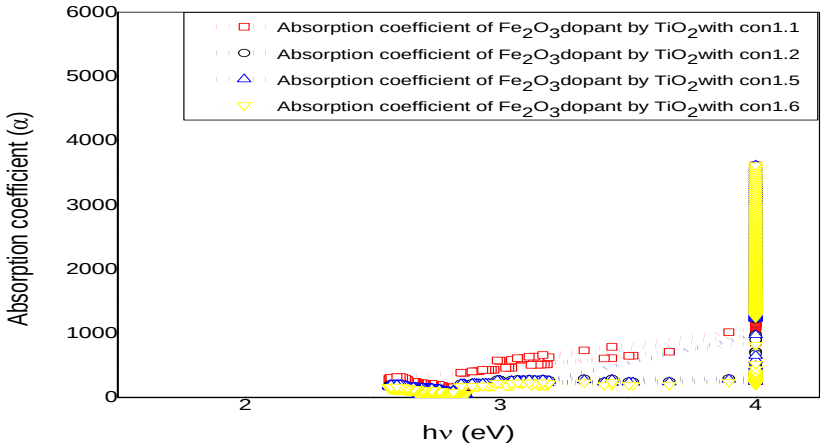

Fig.7.Absorption coefficient vs wavelength plot of Fe_2O_3 doped TiO_2 thin films with concentration (1.1, 1.2, 1.5 and1.6mol/L) at annealing temperature (450^o- 500^o)

There are many different methods for determining the optical band gap (Eg).yadav et al , dghoughi et al, pejova and coworkers , Ismail et al determined the band gap from the relation between the absorption coefficient (α) and the energy incident light $h\nu$

$$(\alpha h\nu)^n = B\,(h\nu - Eg) \qquad \text{.....(3)}$$

Where $h\upsilon$ is the photon energy, B is constant, and n represents the transition type (n = 2) for direct transition n = (½ for indirect transition). The values of direct optical band gap (E_g) values of the TiO_2:Fe_2O_2 thin films were obtained from the intercept of $(\alpha h\nu)^2$vs $h\nu$ curves plotted as shown in figs (8,9,10,11 and 12) from these figures it can notice that the optical band gap decreased from 4.7eV before annealing to (3.9eV , 3.26eV , 3.24eV and 3.27eV) after annealing temperature at(450^o – 500^o) for TiO_2:Fe_2O_3 thin films, this result refer to the broadening of secondary levels that product by TiO_2: doping to the Fe_2O_2thin films.

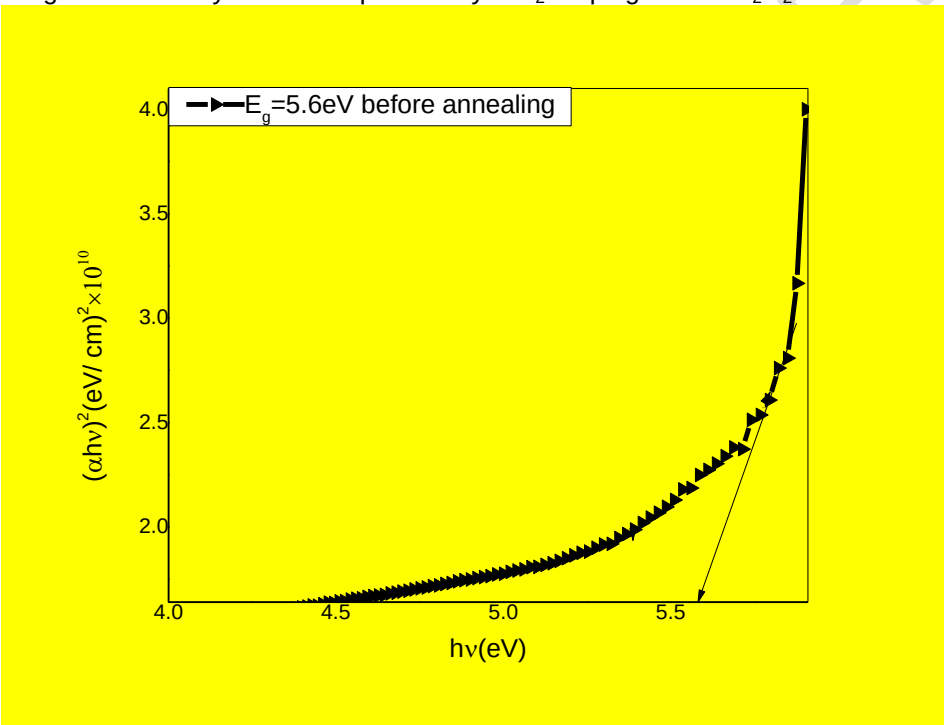

Fig.8. $(\alpha h\nu)^2$ vs $(h\nu)$ plot of TiO_2 thin films before annealing

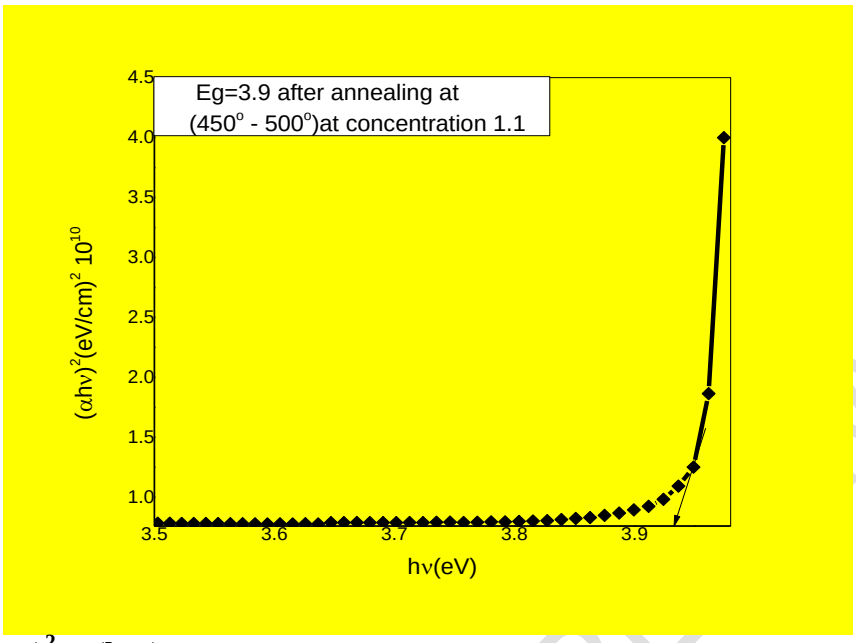

Fig.9. $(\alpha h\nu)^2$vs $(h\nu)$ plot of Fe_2O_3 doped TiO_2 thin films with concentration 1.1mol/L at annealing temperature (450^0- 500^0)

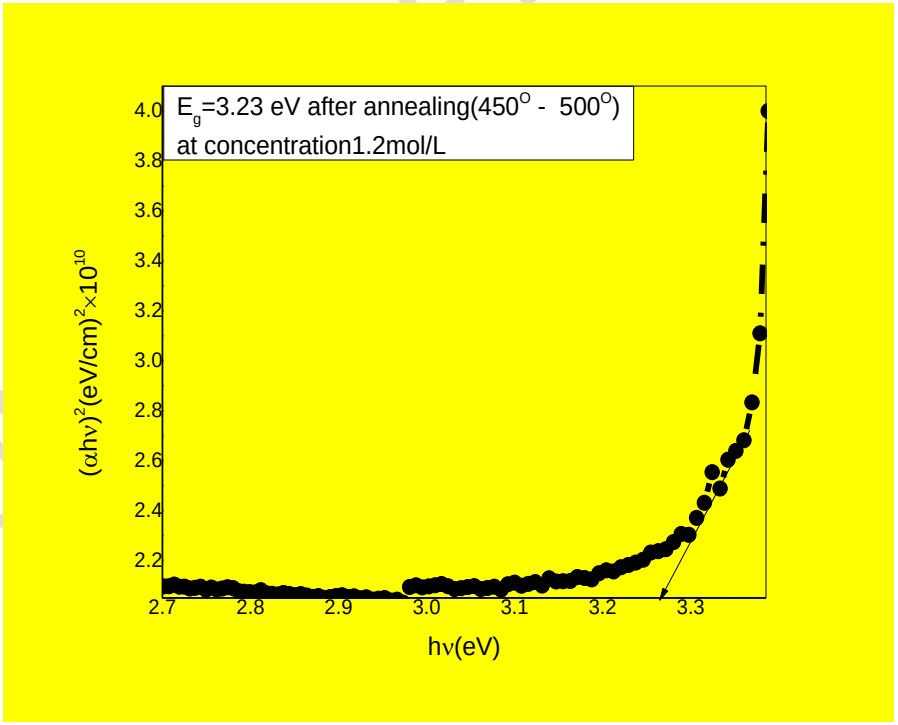

Fig.10. $(\alpha\ h\nu)^2$ vs $(h\nu)$ plot of Fe_2O_3 doped TiO_2 thin films with concentration 1.2mol/L at annealing temperature (450^0- 500^0)

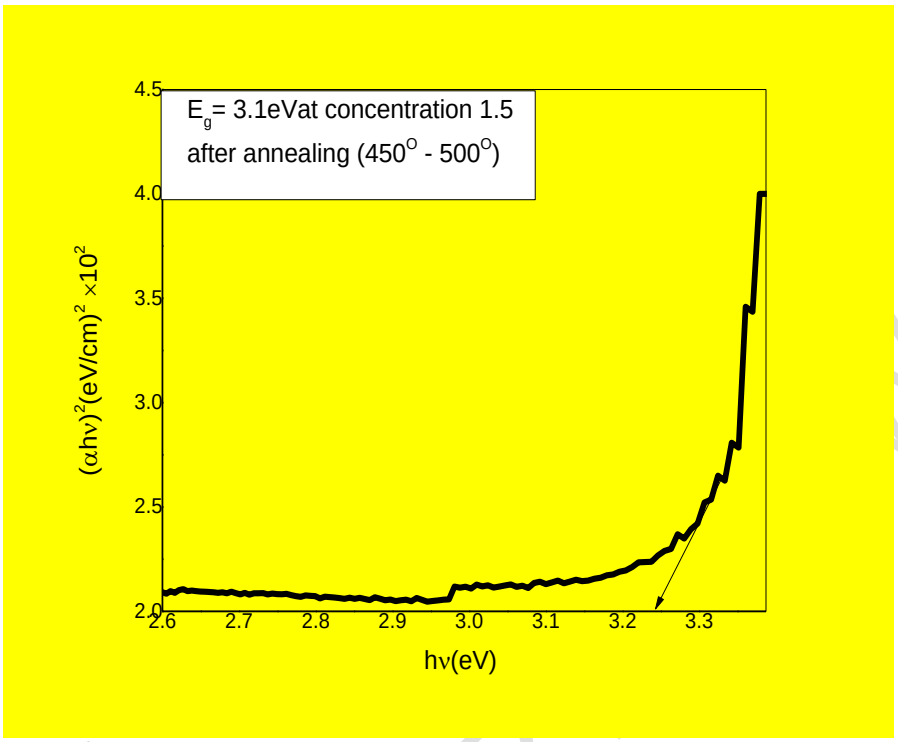

Fig.11. (α $h\nu$)^{2}vs ($h\nu$) plot of Fe_2O_3 doped TiO_2 thin films with concentration 1.5mol/L at annealing temperature (450^0- 500^0)

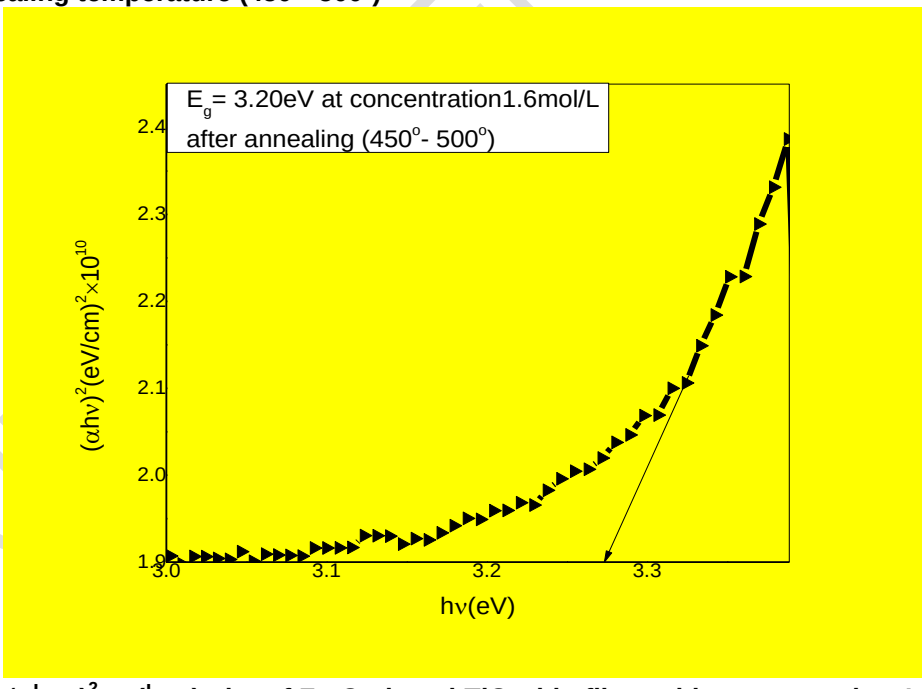

Fig.12. (α$h\nu$)^{2}vs ($h\nu$) plot of Fe_2O_3 doped TiO_2 thin films with concentration 1.6mol/L at annealing temperature (450^0- 500^0)

The refractive index dispersion plays an important role in the research of optical materials because it is a significant factor in optical communication and designing devices for spectral dispersion. The refractive index of the film was calculated approximately from the following relation.

$$R = \frac{(n-1)^2 - k^2}{(n+1)^2 - k^2} \qquad \text{.....(4)}$$

Where n is the refractive index and k is extinction coefficient. Fig (13) shows the variation of refractive index with wavelength for different concentration after annealing temperature at (450^o – 500^o) of TiO_2 : Fe_2O_3 films from this figure , it is clear that n decrease with low concentration and increase with high concentration after annealing temperature that mean the density is decreased of this films.

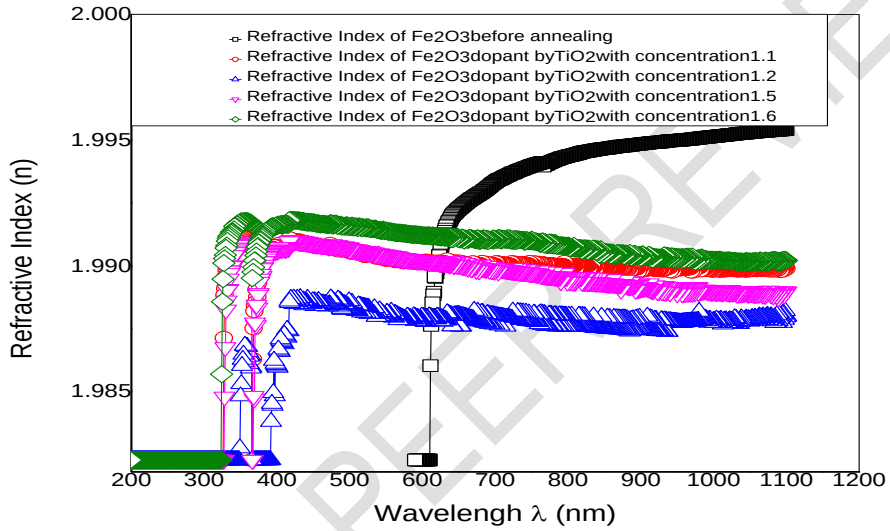

Fig.13. refractive index vs wavelength plot of Fe_2O_3 before and after doped TiO_2 thin films at concentration (1.1, 1.2, 1.5 and 1.6mol/L) at annealing temperature (450^o- 500^o)

Fig (14). Shows the extinction coefficient of TiO_2:Fe_2O_3 thin films before and after annealing with different concentration (1.1, 1.2, 1.5 and 1.6) and in the range of (100 – 1200) nm. It can observe from this figure that the extinction coefficient, decrease sharply with the increase of wavelength for all prepared sample and notice all samples after annealing interfere with each other But the samples before annealing is far from them also before annealing The sample is vertical from the beginning but after annealing there is a slight deviation from the range (4000 – 1000) and then becomes vertically from the range (1000 – 0) then be stable after that range.

The extinction coefficient of the film was calculated approximately from the following relation:

$$k = \frac{A}{C} \qquad \text{..... (5)}$$

Where k the extinction coefficient, A is the absorbance and C is the concentration

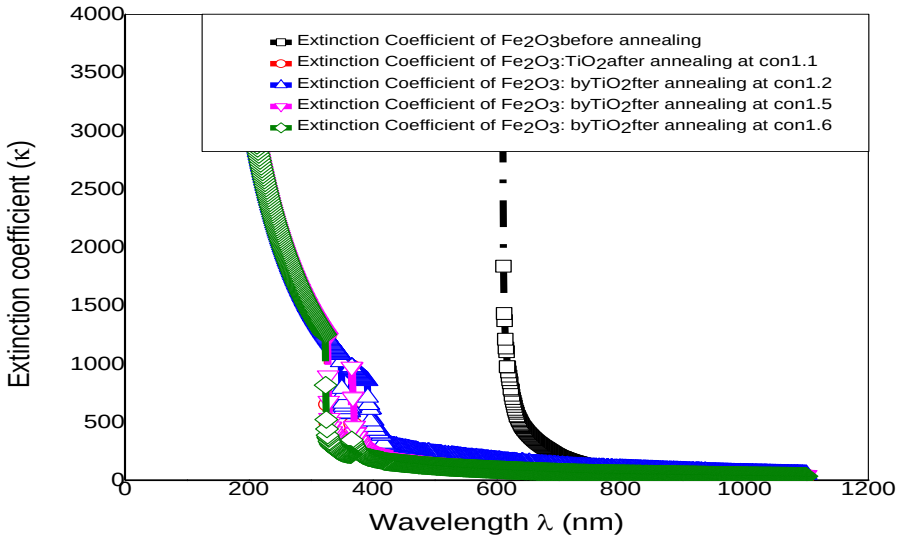

Fig.14. extinction Coefficient vs wavelength plot of Fe_2O_3 doped TiO_2 thin films with concentration (1.1, 1.2, 1.5 and1.6mol/L) at annealing temperature (450^o- 500^o)

4. CONCLUSION

This project is conducted to show that, the annealing of TiO_2 film can increase its efficiency in a DSSC. In this research, the TiO_2 thin film shows better result after annealing; with the increase in temperature during annealing process. Spray pyrolysis deposition method has been selected to produce TiO_2 thin film. By annealing with different temperature, the (450^o to 500^o) is found to be the best temperature for annealing. TiO_2 thin film, based on the optical properties and surface morphology result. For the conclusion, the study concluded that an affect with temperature will increase the efficiency of TiO_2 thin film in DSSC. It also proves that the fabrication of TiO_2 thin films by spray pyrolysis deposition method is successful.

RECOMMENDATIONS:-

The major challenge in the fabrication and commercialization of DSSC is the low conversion efficiency and stability of the cell. The degradation of the cell based on dye sensitization, undesirable electrolyte properties and poor contact with the electrodes are the main causes of the poor performance of DSSC. To enhance the performance of the DSSC is suggested: improving the dye stability by finding the optimum parameters to slow the dye degradation, improving the dye structure to absorb more light at longer wavelengths, 780-2500 nm (the near-infrared region, NIR),improving the morphology of semiconductors to attaining the best electronic conduction to reduce the dark current, using dye and electrolyte additives to enhance the cell performance and improving the mechanical contact between the two electrode. Thus, the choice of materials is very important in the fabrication and deployment of DSSC because the conversion efficiency and stability of the cell do not depend on a single factor alone [4].

REFERENCES

1. Arjunan T V and Senthil T S. Dye sensitized solar cells, Materials Technology, (2013), 28:1-2, 9-14, DOI: 10.1179/1753555712Y.0000000040

2. Qurratulain, Salman Hameed, Safia A. Kazmi, Nadeem Ahmad. “Effect of different dyes on TiO2 based Dye Sensitized Solar Cell”, Department of Electrical Engineering, ZH College of Engineering and Technology, Aligarh Muslim University, Aligarh-202002, India.

3. O’Regan, B.; Gr€atzel, M. Nature 1991, 353, 737.

4. Electrochem Int.J.. Sci., 10 (2015) 2859 – 2871

5. Hagfeldt, A.; Gr€atzel, M. Acc. Chem. Res. 2000, 33, 269.

6. SALAM Z., VIJAYAKUMAR E., SUBRAMANIA A., SIVASANKAR N., MALLICK S., Sol. Energ. Mat. Sol. C., 143 (2015), 250.

7. O’Regan B. C. and Gr¨atzel M., “A low-cost, high-efficiency solarcell based on dye-sensitized colloidal TiO2 films,” Nature,vol. 353, no. 6346, pp. 737–740, 1991.

8. Anta J. A., Guillen E. and Zaera R. T., Phys.Chem J.. C 116, 11413 (2012).

9. Hagfeldt A., Boschloo G., Sun L., Kloo L. and Pettersson H., Chem. Rev. 110, 6595 (2010).

10. GHANN W., KANG H., SHEIKH T., YADAV S.,CHAVEZ-GIL T., NESBITT F., Sci. Rep.-UK, 7 (2017),41470.

11. Fan.Q., Quillion Mc B., Bradley D. D. C., Whitelog S. and Seddon A. B.: ‘A solid state solar cell using sol–gel processed material and a polymer’, Chem. Phys. Lett., 2001, 347, 325–330.

12. Renewable and Sustainable Energy Reviews journalhomepage:www.elsevier.com/locate/rser

13. Giuseppe C. Giuseppe, et al., International journal of molecular sciences, 11 (1) (2010) 254-267.

14. Law. M, Greene L. E., Johnson J. C., Saykally R. and Yang, Nat Mater P., 4 (6) (2005) 455-459.

15. Masayuki Okuya,* Nina A. Prokudina, Katsuya Mushika and Shoji Kaneko, “TiO2 Thin Films Synthesized by the Spray Pyrolysis Deposition (SPD) Technique”, Department of Materials Science and Technology, Shizuoka University 3-5-1 Johoku, Hamamatsu 432-8561, Japan.

16. Masayuki Okuya, Katsuyuki Shiozaki, Nobuyuki Horikawa, Tsuyoshi Kosugi, Asoka Kumara G. R., Janos Madarasz, Shoji Kaneko, Gyorgy Pokol, “Porous TiO2 thin films prepared by spray pyrolysis deposition (SPD) technique and their application to UV sensors”, Departmen of Materials Science and Technology, Shizuoka University, 3-5-1 Johoku, Hamamatsu 432-856, Japan,Research and Development Department, Star Micronics Co., Ltd., 20-10 Nakayoshida, Shizuoka 422-8654, Japan, General and Analytical Chemistry, Budapest University of Technology and Economics, Szt Gellert ter 4, Budapest 1521, Hungary, 2004.

17. European Scientific Journal June 2014 /SPECIAL/ edition vol.2 ISSN: 1857 – 7881 (Print) e - ISSN 1857- 7431